J Therm Anal Calorim (2010) 100:999–1008
DOI 10.1007/s10973-009-0267-1

Crystallization and melting behavior of PP/$CaCO_3$ nanocomposites during thermo-oxidative degradation

Yuhai Wang · Hao Shen · Gu Li · Kancheng Mai

Received: 12 April 2009 / Accepted: 17 June 2009 / Published online: 9 July 2009

Abstract The crystallization and melting behavior of PP/$CaCO_3$ nanocomposites during thermo-oxidative degradation process were studied using differential scanning calorimetry and X-ray diffraction. The results indicated that addition of nano-$CaCO_3$ and compatibilizer significantly reduced the thermo-oxidative stability of PP. Before degradation, thermal aging resulted in an increase in the melting temperature and crystallinity of PP due to the annealing crystallization. Thermo-oxidative degradation decreased the melting temperature and increased melting range, and caused an increase in crystallinity of PP due to the chemi-crystallization. The investigation also indicated that the influence of degradation on the small crystals were much more significant than that on the large ones.

Keywords Crystallization · Nanocomposites · Polypropylene · Thermo-oxidative stability

Introduction

Recently, the thermo-oxidative and photo-oxidative degradation of polypropylene (PP) nanocomposites has been a growing interest issue [1–11]. Golebiewski and Galeski [1] studied the thermo-oxidative and thermal stability of PP/MMT nanocomposite and observed that exfoliated MMT exhibit a strong stabilizing effect on PP due to the lower oxygen permeability. The same tendency was obtained by Bertini et al. [2] and Ramos et al. [3]. However, Qin et al. [6] found that the rate of photo-oxidative degradation of PP/MMT nanocomposites was much faster than that of pure PP, and suggested that the influence of compatibilizer and pristine MMT was primary. Morlat et al. [9–11] also reported that the presence of MMT significantly decreased the induction period of oxidation.

The effect of other nanoparticles on thermo-oxidative and photo-oxidative degradation of PP has also been reported [12–15]. Bikiaris et al. [12] indicated that the multi-walled carbon nanotubes (MWCNT) accelerated the oxidation of PP due to the MWCNT surface carboxylic groups. Zhao and Li [15] found that the incorporation of ZnO nanoparticles increased the photo-oxidative stability of PP due to the superior UV light screening effects offered by ZnO nanoparticles.

However, the thermal stability and photo-oxidative degradation behavior and mechanism PP/$CaCO_3$ nanocomposite have little been reported [16–18]. Recently, Li et al. [16] studied the natural photo-aging degradation of PP, PP/$CaCO_3$ and PP/SiO_2 nanocomposites and observed that PP nanocomposites were much more susceptible to photo-oxidative degradation than unfilled PP. Our previous study [18] also found that addition of nano-$CaCO_3$ accelerated the photo-oxidative degradation of PP.

Although much work has been reported on PP/$CaCO_3$ nanocomposites [19–24], the influence of nano-$CaCO_3$ particles on the thermo-oxidative stability of PP, and the crystallization and melting behavior of PP/$CaCO_3$ nanocomposites during thermal degradation process have not been reported. In our previous work [25, 26], we used three kinds of compatibilizers (PP-g-MA, POE-g-MA and EVA-g-MA) with the same polar groups (MA) but different backbones to modify PP/$CaCO_3$ nanocomposites. The results indicated addition of different compatibilizer results

Y. Wang · H. Shen · G. Li · K. Mai (✉)
Key Laboratory of Polymeric Composites and Functional Materials, the Ministry of Education, Materials Science Institute, School of Chemistry and Chemical Engineering, Sun Yat-sen University, Guangzhou 510275, People's Republic of China
e-mail: cesmkc@mail.sysu.edu.cn

in the formation of different interfacial interaction between PP matrix and nano-$CaCO_3$ particles, and the mechanical properties and crystallization behavior of PP/$CaCO_3$ nanocomposites were dependent on these interfacial interactions. During thermal aging test, the compatibilizers may affect the thermo-oxidative stability of PP/$CaCO_3$ nanocomposites, and the interfacial interaction between PP matrix and nano-$CaCO_3$ will change, further influencing the crystallization and melting behaviors of PP/$CaCO_3$ nanocomposites. Thus in this work, the effect of nano-$CaCO_3$ and compatibilizer on the thermo-oxidative stability of PP, and the crystallization and melting behavior of non-aged, thermal aged and degraded PP and PP/$CaCO_3$ nanocomposites were studied.

Experimental

Materials

Polypropylene (EPS30R), ethylene content 2.87%, MFI = 2.1 g 10 min^{-1} (2.16 kg at 230 °C), containing antioxidant additives, was supplied by Dushanzi Petroleum Chemical, China. Polypropylene grafted with maleic anhydride (PP-g-MA), grafting ratio 1.0%, MFI >15 g 10 min^{-1}; Ethylene-octene copolymer grafted with maleic anhydride (POE-g-MA), grafting ratio 1.1%, MFI = 0.72 g 10 min^{-1}; Ethylene-vinyl acetate copolymer grafted with maleic anhydride (EVA-g-MA), grafting ratio 1.0%, MFI = 2.46 g 10 min^{-1}. The compatibilizers were provided by Guangzhou Lushan Chemical Materials Co. China. Nano-$CaCO_3$ (CC) with particle size: 70–90 nm was obtained from Shiraishi Kogyo Kaisha LTD, Japan.

Specimen preparation

All materials were dried in an oven at 60 °C for 12 h. PP/$CaCO_3$ nanocomposites with and without compatibilizers were prepared using a Berstoff ZE25A corotating twin-screw extruder at 200 °C. The compositions of prepared materials were listed in Table 1. The thin films of about 100 μm in thickness were prepared by compression-molding at 200 °C with a pressure of 10 MPa. The thermal aging test was carried out in an air oven at 130 °C for different time.

Characterization of PP/$CaCO_3$ nanocomposites

Oxidation induction time (OIT) measurement was performed on Perkin–Elmer DSC-7 using open sample holder. The mass of specimens is about 15 mg. Firstly, the specimen was held at 50 °C for 5 min with a nitrogen flow of 50 mL min^{-1}. Subsequently, the specimen was heated to 190 °C at a rate of 20 °C min^{-1} under a flow of nitrogen. After the specimen was held at 190 °C for 5 min, the gas was switched to oxygen at a flow rate of 50 mL min^{-1}. The OIT is the time interval between the initiation of oxygen flow and the onset of the oxidative reaction in the DSC testing. At least three measurements were carried out to determine the OIT values and the scattering of the results were also obtained.

The crystallization and melting behavior of specimens was examined using differential scanning calorimetry (DSC) (Perkin–Elmer DSC-7) under nitrogen atmosphere. The heat flow and temperatures of DSC were calibrated with standard materials, indium and zinc. The mass of specimens is about 5 mg. Specimens were rapidly heated to 220 °C rapidly and melted for 3 min to erase the thermal history, and then cooled down to 50 °C at a rate of 10 °C min^{-1}. The crystallized specimens were re-heated at a rate of 10 °C min^{-1} to investigate the melting behavior of PP.

A Rigaku D/max-2200 VPC X-ray diffractometer with the Cu Kα radiation at a voltage of 40 kV and a current of 30 mA was used for wide angle X-ray diffraction (WAXD) experiments. The scan speed was 4° min^{-1} in a range of 2θ = 5–40° at ambient temperature. The specimens were pre-treated on Perkin–Elmer DSC-7 thermal system, heating from 50 to 220 °C, holding for 3 min, and then cooling to 50 °C.

Results and discussion

Thermo-oxidative stability of PP/$CaCO_3$ nanocomposites

Previous work [25] indicated that nano-$CaCO_3$ particles tend to aggregate in the PP matrix with increasing the particles content due to the large surface tension of nano-$CaCO_3$ particles. When modified by compatibilizers, the

Table 1 The compositions for PP/$CaCO_3$ nanocomposites

Samples	PP (wt%)	$CaCO_3$ (wt%)	PP-g-MA (wt%)	POE-g-MA (wt%)	EVA-g-MA (wt%)
PP	100	–	–	–	–
PP-10	90	10	–	–	–
PP-10a	85	10	5	–	–
PP-10b	85	10	–	5	–
PP-10c	85	10	–	–	5

MA polar group of compatibilizers would associate with the surface of nano-$CaCO_3$ particles by polarity–polarity interaction, resulting in the formation of a core–shell structure in the composites and different interfacial interaction between PP matrix and nano-$CaCO_3$ particles. The mechanical properties and crystallization behavior of PP/$CaCO_3$ nanocomposites were dependent on these interfacial interactions.

Generally, the oxidation induction time (OIT) determined by DSC is used to estimate the content of antioxidant and to evaluate the thermo-oxidative stability of polymeric materials [27]. The higher OIT value indicates the higher thermo-oxidative stability. In this study, the non-aged PP had an OIT value of 33.4 min. The OIT values of extruded and compressed specimens are displayed in Table 2. It can be observed that the OIT of PP decreases after extrusion and compression. The OIT values of extruded and compressed specimens range as: PP > PP-10 > PP-10a > PP-10b > PP-10c. Addition of nano-$CaCO_3$ decreases the thermo-oxidative stability of PP. Addition of compatibilizer decreases the OIT of PP/$CaCO_3$ nanocomposite, indicating that addition of compatibilizer further decreases the thermo-oxidative stability of PP. The decrease of OIT for PP/$CaCO_3$ nanocomposites may be attributed to the consumed antioxidant due to the effect of heat and oxygen [28], and/or the absorption of antioxidant by nano-$CaCO_3$ particles and compatibilizers. The decrease of OIT for compressed thin sample may be also attributed to that oxygen diffusion in a thin film is much faster than that in a bulky sample, which will accelerate the thermo-oxidation of PP matrix.

In order to study the thermo-oxidative degradation of PP and PP/$CaCO_3$ nanocomposites, the specimens were thermally aged at 130 °C for different thermal aging time. The OIT values of these aged specimens are shown in Table 3. It can be seen that the OIT of aged specimens decreases with increasing the thermal aging time. Thermo-oxidative degradation of specimens will begin as the OIT value is zero at which the antioxidants are completely depleted. In this study, the time, at which the OIT value is zero, is considered as the initial oxidation time of the specimens. The higher initial oxidation time indicates the higher thermal-oxidative stability. It can be observed from Table 3 that the initial oxidation time ranges as: PP > PP-10 > PP-10a > PP-10b > PP-10c. It also indicates that addition of nano-$CaCO_3$ and compatibilizer decreases the thermo-oxidative stability of PP.

Table 3 The OIT of aged PP and its nanocomposites

Aging time (h)	OIT (min)				
	PP	PP-10	PP-10a	PP-10b	PP-10c
0	15.9 ± 1.8	12.5 ± 1.3	11.3 ± 1.5	10.6 ± 1.2	8.7 ± 1.0
12	14.8 ± 2.0	10.6 ± 1.5	10.1 ± 1.2	9.8 ± 1.1	7.8 ± 1.3
36	14.5 ± 1.6	10.4 ± 1.2	8.7 ± 1.3	9.2 ± 1.3	7.2 ± 1.3
48	12.9 ± 1.7	8.6 ± 1.4	7.2 ± 0.8	8.3 ± 1.0	6.3 ± 1.1
72	10.8 ± 1.2	6.6 ± 0.9	6.7 ± 1.1	7.5 ± 0.7	5.9 ± 0.8
144	10.5 ± 1.0	4.5 ± 0.4	4.0 ± 0.6	4.3 ± 0.5	3.8 ± 0.2
192	10.2 ± 1.4	3.6 ± 0.5	3.5 ± 0.2	3.2 ± 0.7	1.9 ± 0.3
240	8.0 ± 1.1	2.6 ± 0.2	1.3 ± 0.1	1.7 ± 0.3	–
264	7.5 ± 1.2	2.0 ± 0.3	0.9 ± 0.1	–	–
288	7.1 ± 1.0	1.0 ± 0.1	–	–	–
312	6.5 ± 0.7	–	–	–	–
384	5.8 ± 0.6	–	–	–	–
456	4.7 ± 0.2	–	–	–	–
528	2.1 ± 0.3	–	–	–	–
588	–	–	–	–	–

The effect of filler on the thermo-oxidative or photo-oxidative degradation of PP has been reported by many authors. They suggested that the lower thermo-oxidative or photo-oxidative stabilities of PP composites were attributed to the presence of the metal ions in the MMT [8], the formation of organic salt [3], and addition of compatibilizer [6], and the strong interaction between the stabilizer of PP and the inorganic particles [10, 29].

Addition of nano-$CaCO_3$ decreases the thermo-oxidative stability of PP. It is suggested that the strong interaction among the antioxidant, compatibilizer and nano-$CaCO_3$ results in the decreased content of antioxidant in PP matrix. The lowest OIT of PP-10c is attributed to the strong interaction between the antioxidant and EVA-g-MA with high polar. On the other hand, nano-$CaCO_3$ and compatibilizer act as impurities to accelerate thermo-oxidative degradation of PP. Furthermore, the lower thermo-oxidative stability of PP is also dependent on the spherulite size of PP. The formation of small spherulite size of PP due to the higher nucleation of nano-$CaCO_3$ and compatibilizer would lead to more crystal interface to favor thermo-oxidative degradation [16].

Table 2 The OIT of PP and its nanocomposites

	OIT (min)				
	PP	PP-10	PP-10a	PP-10b	PP-10c
Extruded sample	23.7 ± 2.4	20.0 ± 2.5	15.4 ± 1.8	13.9 ± 1.5	11.1 ± 1.6
Compressed sample	15.9 ± 1.8	12.5 ± 1.3	11.3 ± 1.5	10.6 ± 1.2	8.7 ± 1.0

Crystallization and melting behaviors of aged PP/$CaCO_3$ nanocomposites

With increasing thermal aging time, the OIT value of PP and its nanocomposites decreases and can not be detected when degraded. In this study, the specimen with OIT > 0 is called as aged specimen and the specimen with undetectable OIT is called as degraded specimen. Many investigations [30–33] indicated that thermal aging will change the crystallization and morphology of PP matrix. Figure 1 shows the melting curves of aged PP and PP-10 at 130 °C with different thermal aging time. The melting curves of modified PP/$CaCO_3$ nanocomposites are found to have a similar tendency in nature (figure not shown here). The first melting temperatures and crystallinities of PP are shown in Fig. 2. It can be observed that the melting temperatures and the intensity of lower temperature region increase with thermal aging time and the melting temperatures of PP-10, PP-10a and PP-10b are higher than those of PP and PP-10c. The crystallinities of PP increase and reach a steady value with increasing thermal aging time.

Because of the fast cooling rate during sample preparation process, PP chains did not have sufficient time to crystallize. This makes the existing crystals less perfect and there exists large fraction of amorphous phase in PP matrix. Elevated temperature increases the mobility of the entangled molecule segments in the amorphous region, and makes it easily for these molecule segments to attach to the existing crystals or to form new crystals in the amorphous phase [30]. Thus, the existing crystals become perfect and the crystallinity increases. This process is known as secondary crystallization produced by annealing [34].

The crystallization temperatures of aged specimens are shown in Fig. 3. It can be seen that the crystallization temperature of PP ranges as: PP-10a > PP-10b > PP-10 > PP-10c > PP. For non-aged specimens, addition of nano-$CaCO_3$ increases the crystallization temperature of PP due to the heterogeneous nucleation of nano-$CaCO_3$ and addition of compatibilizers rarely influences the crystallization temperature of PP [26]. However, addition of PP-g-MA further increases the crystallization temperature of PP matrix in PP/$CaCO_3$ nanocomposite. It is suggested that the polar groups (MA) of compatibilizer react with nano-$CaCO_3$ particles to form carboxylate salts which can act as a more effective nucleating agent and induce the formation of β-crystal of PP. However, the nucleation effect of carboxylate salts depends on the compatibility between PP and compatibilizer. The high compatibility between PP and PP-g-MA favors the nucleation of carboxylate salts. For PP-10b, the nucleation effect of carboxylate salts is weakened because of the weak compatibility between PP and POE-g-MA. For PP-10c, the incompatibility between PP and EVA-g-MA retards the nucleation effect of carboxylate salts. The

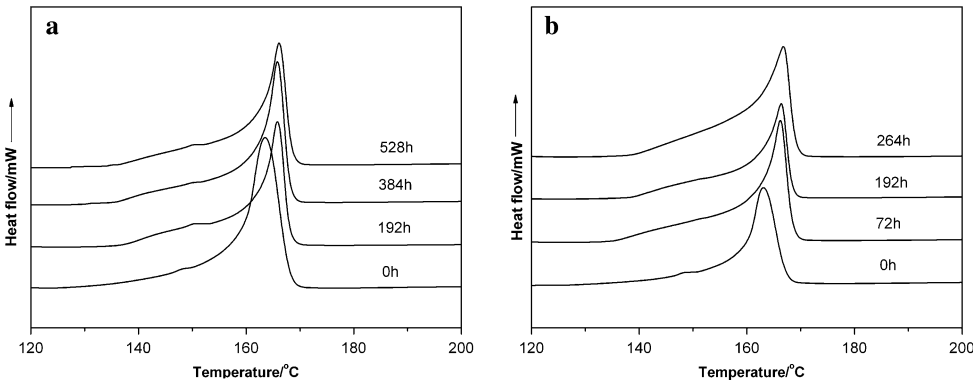

Fig. 1 First melting curves of **a** aged PP and **b** aged PP-10 at different thermal aging time

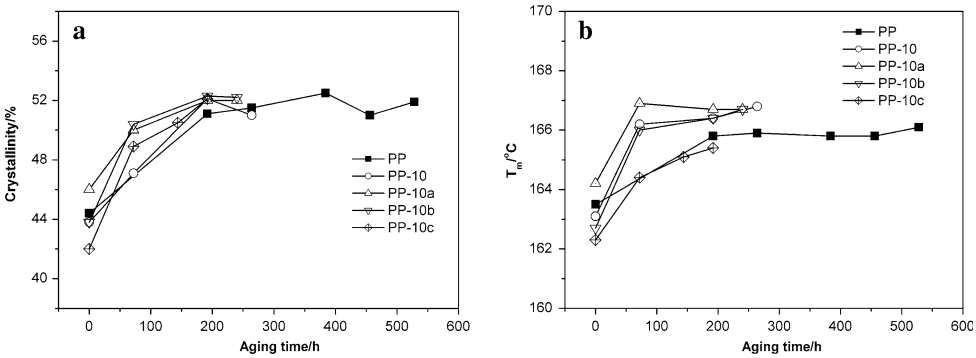

Fig. 2 DSC **a** first melting temperatures and **b** crystallinities of aged specimens as a function of thermal aging time

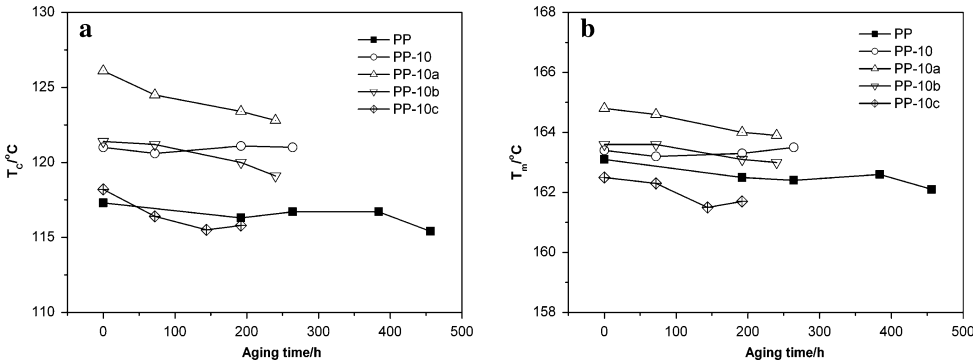

Fig. 3 DSC **a** crystallization temperatures and **b** second melting temperatures of aged specimens as a function of thermal aging time

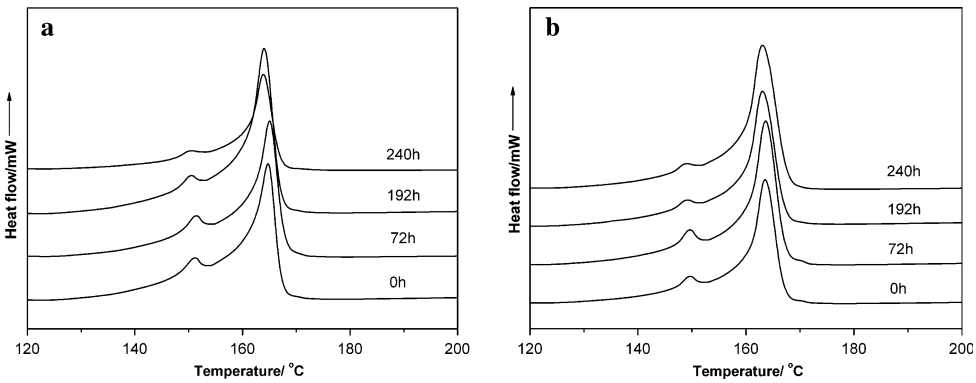

Fig. 4 Second melting curves of **a** aged PP-10a and **b** aged PP-10b at different thermal aging time

spherulites size of these specimens ranges as: PP > PP-10c > PP-10 > PP-10b > PP-10a.

It can be observed from Fig. 3 that the decrease of the crystallization temperatures for modified PP/$CaCO_3$ nanocomposites is more significant than that of PP and PP/$CaCO_3$ nanocomposite with increasing thermal aging time. It may be attributed that the carboxylate salts is susceptible to be affected by heat and oxygen, and/or that thermal aging results in the lower compatibility between PP and compatibilizer, weakening the nucleation effect of carboxylate salts.

The second melting temperatures of aged specimens show the similar tendency of crystallization temperature (Fig. 3b). The specimens with high crystallization temperatures exhibit high melting temperatures. Addition of PP-g-MA and POE-g-MA induced the formation of β-crystal in the PP/$CaCO_3$ nanocomposites (Fig. 4). However, the intensity of melting peak for β-crystal of PP decreases with increasing thermal aging time. This also indicates that thermal aging weakens the nucleation effect of carboxylate salts.

Crystallization and melting behaviors of degraded PP/$CaCO_3$ nanocomposites

Thermo-oxidative degradation of specimens occurs as the antioxidant was depleted during thermal aging process. The melting curves of degraded specimens are shown in Fig. 5. As compared, the melting curves of non-aged and aged specimens are also displayed in these graphs. It can be observed that the melting curves of degraded specimens are different from those of aged specimens. On the other hand, the melting curves of degraded PP and PP-10 are different from those of degraded PP/$CaCO_3$ nanocomposites modified by compatibilizers. Double melting peaks for degraded PP and PP-10 and three melting peaks for degraded PP/$CaCO_3$ nanocomposites modified by compatibilizers are observed. For degraded PP, PP-10 and PP-10c, the intensity of high-temperature melting peak is higher than that of low-temperature melting peak. For degraded PP-10a and PP-10b, the intensity of low-temperature melting peak is higher than that of high-temperature melting peak, especially for PP-10a.

We can see from Fig. 5 that the high-temperature peaks in degraded specimens show similar temperatures with those in original specimens, in another word, annealing increases the melting temperatures but degradation decreases them. It seems likely that the perfection of the crystals by annealing is destroyed by degradation. This suggests that the molecule segments attaching to the existing crystals during annealing are unstable and are easily attacked by oxidation, which is similar to the investigation by Elvira et al. [32] that the highest temperature component was mostly due to non-equilibrium

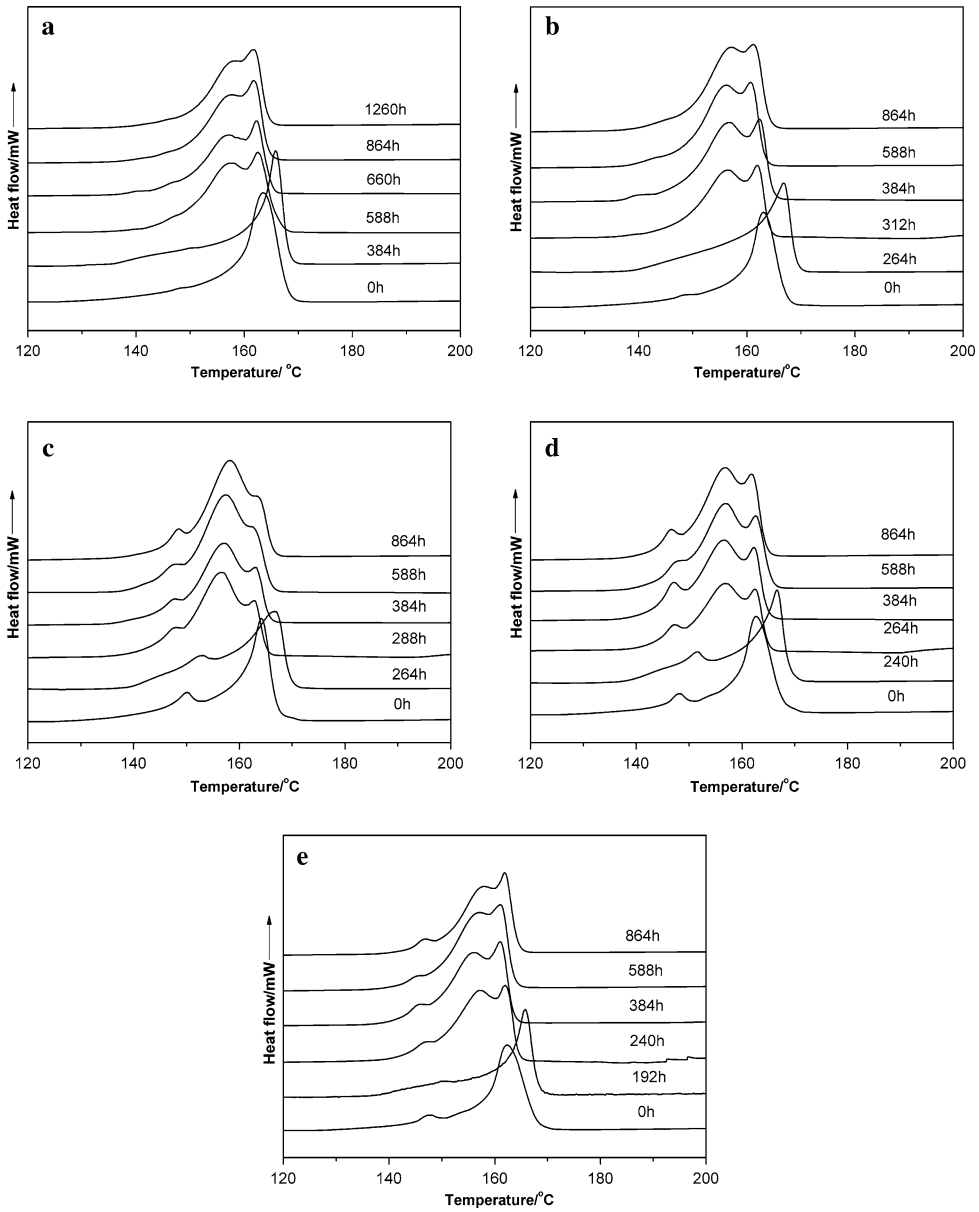

Fig. 5 First melting curves of degraded specimens at different thermal aging time: **a** PP, **b** PP-10, **c** PP-10a, **d** PP-10b and **e** PP-10c

associations during thermal aging, and were destroyed when degradation spreaded out.

The half-widths of melting peaks (melting ranges) from the DSC curves are displayed in Fig. 6. The melting range of PP first decreases and later significantly increases with increasing thermal aging time. It is generally considered that the melting range is related to the distribution of crystal thickness and/or perfection of PP. The narrower is the melting range, the more uniform are the crystals within the material [35]. Before degradation, the decrease in melting range is attributed to the increase in the perfection of existing crystals by thermal annealing. Once the thermal oxidation degradation began, the crystals with different perfection were formed, resulting in the increased melting range [36] and the occurrence of multi-melting peaks of PP. The thermal aging time in the sharp increase of melting range also indicated that the thermo-oxidative stability is PP $\gg$ PP/$CaCO_3$ nanocomposite $>$ modified PP/$CaCO_3$ nanocomposites.

The melting temperatures and crystallinities of degraded specimens are shown in Fig. 7. Although thermal aging increases the melting temperature of PP, the melting temperatures of PP sudden decrease once degraded. This result indicates that the thermo-oxidative degradation decreases the crystal thickness and/or perfection of PP. The increased crystallinity (about 5–10%) of degraded specimens is attributed to the chemi-crystallization [36].

As generally accepted, degradation reaction of semi-crystalline polymers proceed predominantly in amorphous regions because of the higher permeability to oxygen and

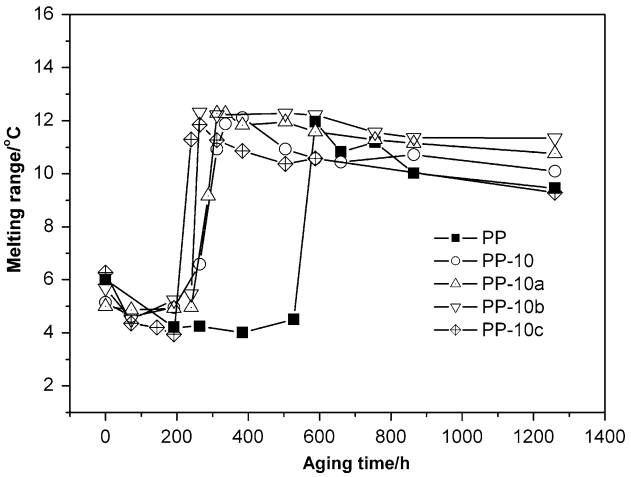

Fig. 6 Melting ranges of the specimens as a function of thermal aging time

the higher concentration of impurities. Degradation reaction will cause the chain scissions, which releases the chain segments that were previously entangled and were not able to crystallize during the original crystallization process or during the annealing process. These segments, with an appreciable mobility, will attach to the growth faces of pre-existing crystals nearby or to form new crystals in the amorphous phase. This will increase the crystallinity and is often known as chemi-crystallization [36]. Degradation may also occur at the lamellar fold surfaces, resulting in a reduction of the melting temperature [37]. Rabello and White [37] demonstrated that the decrease of the melting temperature in a sample with large lamellar thickness is much less significant than in a sample with small lamellar thickness. Thus, for PP and PP-10c, the crystals with large sizes, which are dominant in the specimens, suffer less degradation than the small ones and still show the main peak on the melting thermograms (Fig. 5a, e). On the other hand, the small crystals are dominant in PP-10a and PP-10b. These small crystals suffer more severe degradation than the lager one, their melting temperatures decrease and show a main peak at lower temperature (Fig. 5c, d), especially for PP-10a in which the crystals is the smallest.

The crystallization temperatures, second melting temperatures and crystallinities of degraded specimens are shown in Fig. 8. Once degraded, all these parameters show a sudden decrease in a very short time and then reach a steady value. The decrease of the crystallization temperatures is presumably attributed to the destruction of carboxylate salts and/or the formation of larger number of chemical irregularities of molecular chain of degraded PP [38] resulting in the decreased heterogeneous nucleation of nano-$CaCO_3$ particles and compatibilizer, which is proved by the disappearance of β-crystals in PP-10a and PP-10b (Fig. 9). The reduction in the second melting temperature of degraded specimens is attributed to that the recrystallized specimens contain molecules that are both smaller and defective. The decrease in the crystallinities of recrystallized specimens is caused by that the highly degraded molecules are not able to crystallize during cooling. As seem in Fig. 8c, the specimens containing large crystals (PP and PP-10c) display less reduction in crystallinities and have higher crystallinities than the ones containing small crystals (PP-10, PP-10a and PP-10b). The degraded specimen will always contain a significant fraction of crystallizable polymer in the form of short segments that come from the crystals, which remain undamaged during exposure [36]. Thus, it seems that the large crystals suffer less degradation and contain more undamaged molecules than the small crystals.

The second melting curves of PP and PP-10 are shown in Fig. 10. The melting peaks shift to low temperatures when degraded. Small shoulder peaks at high temperature exhibit shortly after the beginning of degradation and disappear when increase the thermal aging time. The presence of shoulder peaks indicates the different characteristics crystals (e.g. different degree of perfection) exist in degraded specimens due to the recrystallization of various damaged molecules. When degradation spreads out, the disappearance of shoulder peaks may be attributed to the co-crystallization of various damaged molecules [35] or the only recrystallization of the undamaged molecular segments, which result in uniform crystals in the recrystallized specimens.

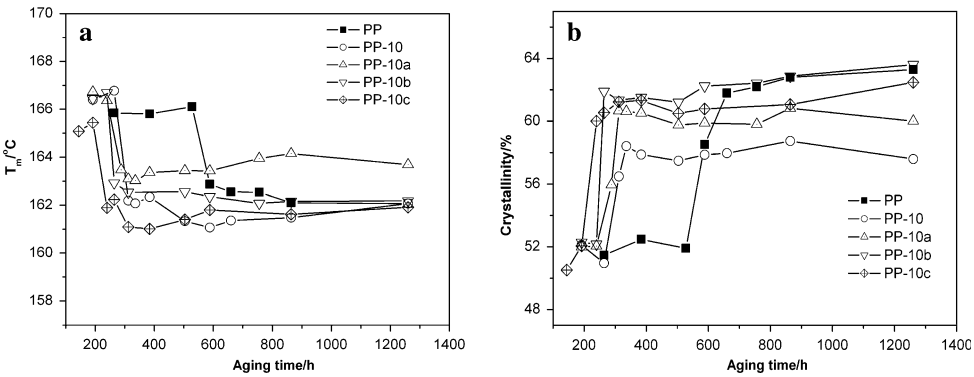

Fig. 7 DSC **a** first melting temperatures and **b** crystallinities of degraded specimens as a function of thermal aging time

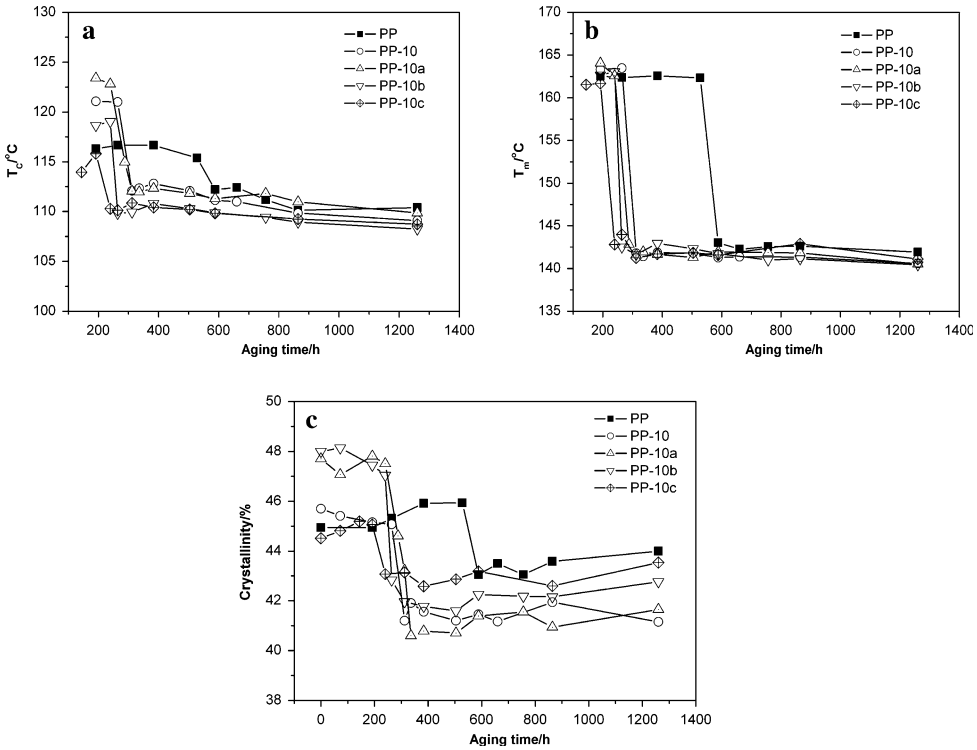

Fig. 8 DSC **a** crystallization temperatures, **b** second melting temperatures and **c** crystallinities of degraded specimens as a function of thermal aging time

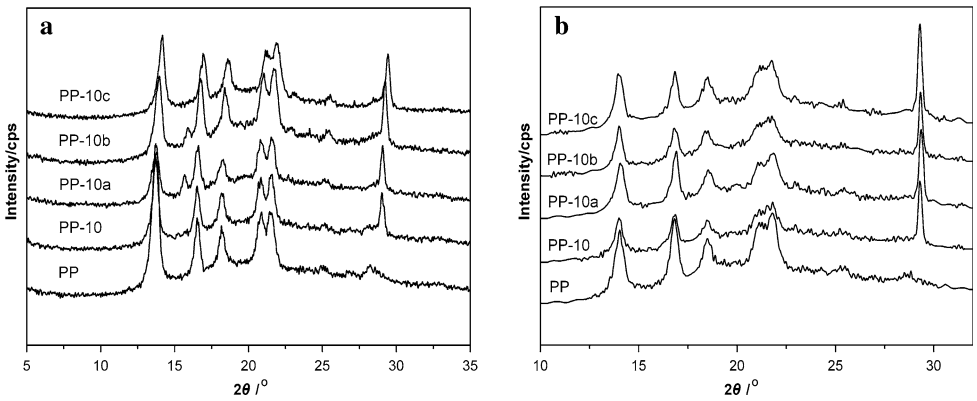

Fig. 9 WAXS patterns of **a** non-aged and **b** degraded specimens at the thermal aging time of 864 h

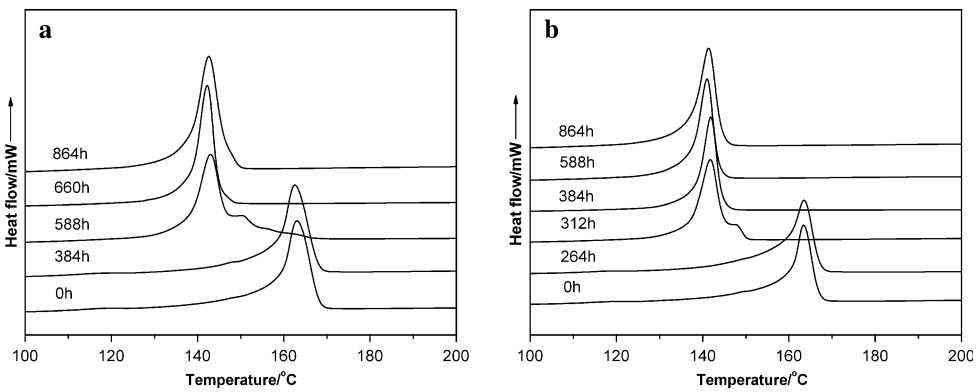

Fig. 10 Second melting curves of **a** PP and **b** PP-10 at different thermal aging time

The crystallization ranges (the half-widths of DSC crystallization peaks) is generally used to estimate the crystallizability of polymers. It can be seen from Fig. 11 that the crystallization ranges of non-aged PP-10, PP-10a and PP-10b are lower than that of PP and PP-10c due to the higher nucleation. Once degraded, the crystallization

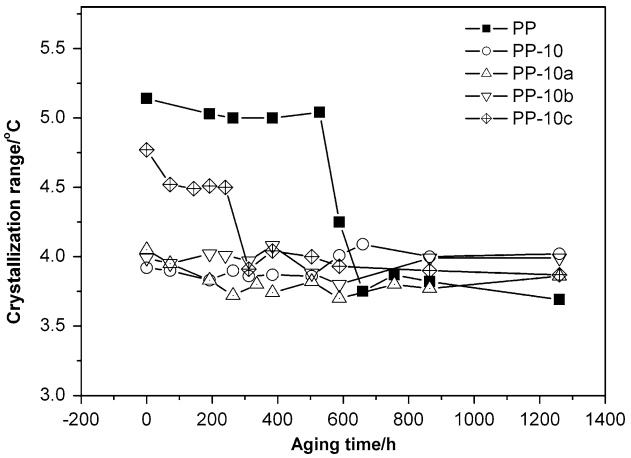

Fig. 11 Crystallization ranges of the specimens as a function of thermal aging time

ranges of PP and PP-10c sudden decrease to the same as that of PP-10, PP-10a and PP-10b. Generally, it is considered that thermo-oxidative degradation will result in the decrease of crystallization rate and the increase of crystallization ranges. However, it is not the case. It is suggested that the thermo-oxidative degradation of PP decreases the molecular weight and increases the crystallization rate of PP in degraded PP and PP-10c.

Conclusions

The effect of nano-$CaCO_3$ and compatibilizer on thermal-oxidative stability of PP and the crystallization and melting behavior of PP/$CaCO_3$ nanocomposites during thermal aging were investigated. The results indicated that addition of nano-$CaCO_3$ and compatibilizer significantly decreased the oxidation induction time of PP. Before thermo-oxidative degradation, thermal aging increased the melting temperature and crystallinity of PP due to the annealing crystallization, and decreased the crystallization temperature of modified nanocomposites due to the decreased nucleation effect of nano-$CaCO_3$ and compatibilizer. Thermo-oxidative degradation resulted in the decrease in melting temperature and the increase in melting range, and caused an increase in crystallinity of PP due to the chem-crystallization. All the oxidation induction time, melting temperature, crystallization temperature, melting range and crystallinity indicated that addition of nano-$CaCO_3$ decreased the thermal-oxidative stability of PP. Addition of compatibilizer further decreased the thermal-oxidative stability of PP. The investigation also indicated that the influence of degradation on the small crystals were much more significant than that on the large ones.

Acknowledgements The project was supported by Natural Science Foundation of China (Grant No. 50873115), Doctoral Fund of Ministry of Education of China and Project of Science and Technology of Guangdong Province, China (Grant No. 0711020600002).

References

1. Golebiewski J, Galeski A. Thermal stability of nanoclay polypropylene composites by simultaneous DSC and TGA. Compos Sci Technol. 2007;67:3442–7.
2. Bertini F, Canetti M, Audisio G, Costa G, Falqui L. Characterization and thermal degradation of polypropylene-montmorillonite nanocomposites. Polym Degrad Stab. 2006;91:600–5.
3. Ramos FFG, Melo TJA, Rabello M, Silva SML. Thermal stability of nanocomposites based on polypropylene and bentonite. Polym Degrad Stab. 2005;89:383–92.
4. Qin HL, Zhang SM, Zhao CG, Hu GJ, Yang MS. Flame retardant mechanism of polymer/clay nanocomposites based on polypropylene. Polymer. 2005;46:8386–95.
5. Qin HL, Zhang SM, Zhao CG, Feng M, Yang MS, Shu ZJ, et al. Thermal stability and flammability of polypropylene/montmorillonite composites. Polym Degrad Stab. 2004;85:807–13.
6. Qin HL, Zhang SM, Liu HJ, Xie SB, Yang MS, Shen DY. Photooxidative degradation of polypropylene/montmorillonite nanocomposites. Polymer. 2005;46:3149–56.
7. Diagne M, Gueye M, Vidal L, Tidjani A. Thermal stability and fire retardant performance of photo-oxidized nanocomposites of polypropylene-graft-maleic anhydride/clay. Polym Degrad Stab. 2005;89:418–26.
8. Diagne M, Gueye M, Dasilva A, Tidjani A. Comparative photooxidation under natural and accelerated conditions of polypropylene nanocomposites produced by extrusion and injection molding. J Appl Polym Sci. 2007;105:3787–93.
9. Morlat S, Mailhot B, Gonzalez D, Gardette JL. Photo-oxidation of polypropylene/montmorillonite nanocomposites. 1. Influence of nanoclay and compatibilizing agent. Chem Mater. 2004;16:377–83.
10. Morlat S, Mailhot B, Gonzalez D, Gardette JL. Photooxidation of polypropylene/montmorillonite nanocomposites. 2. Interactions with antioxidants. Chem Mater. 2005;17:1072–8.
11. Mailhot B, Morlat S, Gardette JL, Boucard S, Duchet J, Gerard JF. Photodegradation of polypropylene nanocomposites. Polym Degrad Stab. 2003;82:163–7.
12. Bikiaris D, Vassiliou A, Chrissafis K, Paraskevopoulos KM, Jannakoudakis A, Docoslis A. Effect of acid treated multi-walled carbon nanotubes on the mechanical, permeability, thermal properties and thermo-oxidative stability of isotactic polypropylene. Polym Degrad Stab. 2008;93:952–67.
13. Du ML, Guo BC, Liu MX, Jia DM. Thermal decomposition and oxidation aging behaviour of polypropylene/halloysite nanotube nanocomposites. Polym Polym Compos. 2007;15:321–8.
14. Gao XW, Meng XF, Wang HT, Wen B, Ding YF, Zhang SM, et al. Antioxidant behaviour of a nanosilica-immobilized antioxidant in polypropylene. Polym Degrad Stab. 2008;93:1467–71.
15. Zhao HX, Li RKY. A study on the photo-degradation of zinc oxide (ZnO) filled polypropylene nanocomposites. Polymer. 2006;47:3207–17.
16. Li JF, Yang R, Yu J, Liu Y. Natural photo-aging degradation of polypropylene nanocomposites. Polym Degrad Stab. 2008;93:84–9.
17. Zaharescu T, Jipa S, Kappel W, Supaphol P. The control of thermal and radiation stability of polypropylene containing calcium carbonate nanoparticles. Macromol Symp. 2006;242:319–24.

18. Wang YH, Shen H, Mai KC. FT-IR study on the photo-oxidative degradation of nano-$CaCO_3$/PP composites. Acta Scientiarum Naturalium Universitatis Sunyatseni. 2008;47:62–6.
19. Lin ZD, Huang ZZ, Zhang Y, Mai KC, Zeng HM. Crystallization and melting behavior of nano-$CaCO_3$/polypropylene composites modified by acrylic acid. J Appl Polym Sci. 2004;91:2443–53.
20. Lin ZD, Zhang ZS, Huang ZZ, Mai KC. Investigation on preparation and property of nano-$CaCO_3$/PP masterbatch modified by reactive monomers. J Appl Polym Sci. 2006;101:3907–14.
21. Avella M, Cosco S, Di Lorenzo ML, Di Pace E, Errico ME. Influence of $CaCO_3$ nanoparticles shape on thermal and crystallization behavior of isotactic polypropylene based nanocomposites. J Therm Anal Calorim. 2005;80:131–6.
22. Chan CM, Wu JS, Li JX, Cheung YK. Polypropylene/calcium carbonate nanocomposites. Polymer. 2002;43:2981–92.
23. Ma CG, Mai YL, Rong MZ, Ruan WH, Zhang MQ. Phase structure and mechanical properties of ternary polypropylene/elastomer/nano-CaCO3 composites. Compos Sci Technol. 2007;67:2997–3005.
24. Thio YS, Argon AS, Cohen RE, Weinberg M. Toughening of isotactic polypropylene with $CaCO_3$ particles. Polymer. 2002;43:3661–74.
25. Wang YH, Shen H, Li G, Mai KC. Effect of interfacial interaction on the crystallization and mechanical properties of PP-nano-$CaCO_3$ composites modified by compatibilizers. J Appl Polym Sci. 2009;113:1584–92.
26. Wang Y, Shen H, Li G, Mai K. Crystallization and melting behavior of PP/nano-$CaCO_3$ composites with different interfacial interaction. J Therm Anal Calorim. 2009. doi:10.1007/s10973-009-0130-4
27. Woo L, Khare AR, Sandford CL, Ling MTK, Ding SY. Relevance of high temperature oxidative stability testing to long term polymer durability. J Therm Anal Calorim. 2001;64:539–48.
28. Camacho W, Karlsson S. Assessment of thermal, thermo-oxidative stability of multiextruded recycled PP, HDPE and a blend thereof. Polym Degrad Stab. 2002;78:385–91.
29. Hu XZ, Xu HM, Zhang ZF. Influence of fillers on the effectiveness of stabilizers. Polym Degrad Stab. 1994;43:225–8.
30. Litvinov VM, Soliman M. The effect of storage of poly(propylene) pipes under hydrostatic pressure and elevated temperatures on the morphology, molecular mobility and failure behaviour. Polymer. 2005;46:3077–89.
31. Aaron L, Leonardo S, Pearl LS. Effects of thermal aging on isotactic polypropylene crystallinity. Polym Eng Sci. 2008;48:627–33.
32. Elvira M, Tiemblo P, Gomez-Elvira JM. Changes in the crystalline phase during the thermo-oxidation of a metallocene isotactic polypropylene. A DSC study. Polym Degrad Stab. 2004;83:509–18.
33. Guisandez J, Tiemblo P, Gomez-Elvira JM. Change of thermal and dynamic-mechanical behaviour of a metallocene isotactic polypropylene during low-temperature thermo-oxidation. Polym Degrad Stab. 2005;87:543–53.
34. Dudic D, Djokovic V, Kostoski D. The high temperature secondary crystallisation of aged isotactic polypropylene. Polym Test. 2004;23:621–7.
35. Rabello MS, White JR. Photodegradation of talc-filled polypropylene. Polym Compos. 1996;17:691–704.
36. Rabello MS, White JR. Crystallization and melting behavior of photodegraded polypropylene-I. Chemi-crystallization. Polymer. 1997;38:6379–87.
37. Rabello MS, White JR. The role of physical structure and morphology in the photodegradation behaviour of polypropylene. Polym Degrad Stab. 1997;56:55–73.
38. Rabello MS, White JR. Crystallization and melting behaviour of photodegraded polypropylene-II. Re-crystallization of degraded molecules. Polymer. 1997;38:6389–99.